THE JOURNAL OF COMPARATIVE NEUROLOGY 466:513–524 (2003)

Crossed and Uncrossed Retinal Projections to the Hamster Circadian System

LOUISE MUSCAT,[1] ANDREW D. HUBERMAN,[2] CYNTHIA L. JORDAN,[3] AND LAWRENCE P. MORIN[1,4]*

[1]Graduate Program in Neurobiology and Behavior, State University of New York at Stony Brook, Stony Brook, New York 11794

[2]Center for Neuroscience, University of California, Davis, Davis, California 95616

[3]Department of Psychology and Neuroscience Program, Michigan State University, East Lansing, Michigan 48824

[4]Department of Psychiatry, State University of New York at Stony Brook, Stony Brook, New York 11794

ABSTRACT

The hamster suprachiasmatic nucleus (SCN), site of the circadian clock, has been thought to be equally and completely innervated by each retina. This issue was studied in animals that had received an injection of the tracer cholera toxin subunit B (CTb) conjugated to Alexa 488 into the vitreous of one eye, with CTb-Alexa 594 injected into the other. Retinal projections to the SCN and other nuclei of the circadian system were simultaneously evaluated by using confocal laser microscopy. Each retina provides completely overlapping terminal fields throughout each SCN. Although SCN innervation by the contralateral retina is slightly denser than that from the ipsilateral retina, there are distinct SCN regions where input from one side is predominant, but not exclusive. A dense terminal field from the contralateral retina encompasses, and extends dorsally beyond, the central SCN subnucleus identified by calbindin-immunoreactive neurons. Surrounding the dense terminal field, innervation is largely derived from the ipsilateral retina. The densest terminal field in the intergeniculate leaflet is from the contralateral retina, which completely overlaps the ipsilateral projection. Most nuclei of the pretectum receive innervation largely, but not solely, from the contralateral retina, although the olivary pretectal nucleus has very dense patches of innervation derived exclusively from one retina or the other. Retina-dependent variation in terminal field density within the three closely examined nuclei may indicate areas of specialized function not previously appreciated. This issue is discussed in the context of the melanopsin-containing retinal ganglion cell projections to several nuclei in the circadian visual system. J. Comp. Neurol. 466:513–524, 2003.

Indexing terms: suprachiasmatic nucleus; intergeniculate leaflet; olivary pretectal nucleus

The "circadian visual system" enables endogenous 24-hour rhythms to synchronize with the environmental photoperiod. The suprachiasmatic nucleus (SCN), site of the circadian clock, receives photic input directly from the retina via the retinohypothalamic tract (RHT; Moore and Lenn, 1972; Hendrickson et al., 1972; Groos et al., 1983; Groos and Meijer, 1985; Meijer et al., 1986), and an intact RHT is necessary for circadian rhythm entrainment to the environmental photoperiod (Johnson et al., 1988a).

The thalamic intergeniculate leaflet (IGL) is part of the retinorecipient lateral geniculate complex (Card and Moore, 1982, 1989; Harrington et al., 1985, 1987; Morin et al., 1992; Moore and Card, 1994; Morin and Blanchard, 1995, 1997, 1998, 1999, 2001). It provides a major

Grant sponsor: National Institute of Neurological Disorders and Stroke; Grant number: NS22168; Grant sponsor: National Institute of Mental Health; Grant number: MH64471 (L.P.M.); Grant sponsor: National Science Foundation; Grant number: IBN-9818425; Grant number: IBN-0296060 (C.L.J).

*Correspondence to: Lawrence P. Morin, Department of Psychiatry, Health Science Center, Stony Brook University, Stony Brook, NY 11794-8101. E-mail: lmorin@epo.som.sunysb.edu

Received 27 March 2003; Revised 21 May 2003; Accepted 30 June 2003

DOI 10.1002/cne.10894

Published online the week of October 6, 2003 in Wiley InterScience (www.interscience.wiley.com).

projection to the SCN via the geniculohypothalamic tract (GHT), an indirect route by which photic information can gain access to the circadian clock (Zhang and Rusak, 1989). The IGL contributes substantially to the effect of constant light on circadian period length (Harrington and Rusak, 1986; Pickard et al., 1987; Morin and Pace, 2002) and modifies entrainment (Johnson et al., 1989; Pickard, 1989) and phase response to photic signals (Harrington and Rusak, 1986; Pickard et al., 1987). A presently unknown portion of the pretectum or deep superior colliculus also contributes to photic and nonphotic regulation of circadian rhythmicity (Marchant and Morin, 1999).

Both retinas project to the SCN, IGL, and pretectum, although in most regions the ipsi- and contralateral contributions are unequal. Retinal projections to the contralateral pretectal nuclei are much denser than ipsilateral projections (Morin and Blanchard, 1997), but there has not been any analysis of regional specificity to ipsi- and contralateral retinal terminal fields. Retinal projections to the contralateral IGL have been described as being denser than those to the ipsilateral IGL in both rats and hamsters (Hickey and Spear, 1976; Morin et al., 1992). The crossed projection to the SCN is denser than the uncrossed projection in most species, but this is not universal. In some squirrel species, there is no ipsilateral projection (Agarwala et al., 1989; Smale et al., 1991). In certain primates, the ipsilateral projection is denser (Moore, 1973; Magnin et al., 1989; Smale and Boverhof, 1999). For the nocturnal golden hamster and the diurnal *Octodon degus*, the retina has been thought to project equally to each SCN (Johnson et al., 1988b; Goel et al., 1999).

Increasingly sensitive methods have been used as the retinohypothalamic tract has been repeatedly evaluated: autoradiography (Moore and Lenn, 1972; Eichler and Moore, 1974; Card and Moore, 1984); horseradish peroxidase (Johnson et al., 1988b); and cholera toxin B (CTb) subunit immunohistochemistry (Morin and Blanchard, 1999). Until recently, however, such studies employed one monocular injection of anterograde tract tracer, an approach that precludes direct and accurate comparison of inputs from the two eyes.

The SCN, IGL, and pretectum have a recently discovered common feature, in that all three regions receive dense projections from photosensitive retinal ganglion cells containing the putative photopigment melanopsin (Provencio et al., 1998; Hannibal et al., 2002; Berson et al., 2002; Hattar et al., 2002; Morin et al., 2003; Gooley and Saper, 2003). In addition, the hamster SCN, IGL, and pretectum have regionally specialized anatomical features exemplified by specific distributions of various neuron phenotypes (Morin et al., 1992; Miller et al., 1996; Morin and Blanchard, 1997, 2001). This is most obvious in the hamster SCN, where a central subnucleus consisting of at least three cell types is surrounded by regions containing several other fairly discrete collections of peptide-containing cells (Miller et al., 1996).

Resolution of details related to the spatial overlap of binocular retinal projections requires simultaneous use of two easily distinguishable, highly sensitive tracers. Here, we have employed a variation on the very sensitive, high-resolution CTb immunohistochemical method and injected each eye with CTb preconjugated to a different fluorophore. This procedure, combined with thin digital optical sections obtained with confocal laser scanning microscopy, permits clear evaluation of the retinal innervation provided by each eye (Muir-Robinson et al., 2002; Huberman et al., 2002; Stellwagen and Shatz, 2002). The present analysis is a necessary foundation for future determination of the extent to which the neuronal phenotypes in the SCN, IGL, and pretectum are differentially innervated by each retina and whether the melanopsin-containing ganglion cells contribute to functionally specialized parts of each region.

MATERIALS AND METHODS

Outbred adult male Syrian hamsters (N = 27; Charles River Laboratories, Wilmington, MA; 90–100 g bw) were housed in individual cages under a 14-hr-light, 10-hr-dark photoperiod with free access to food and water for 15–21 days before use. Each animal was then deeply anesthetized with intraperitoneal sodium pentobarbital (Abbott Laboratories, North Chicago, IL; 100 mg/kg) and placed in a stereotaxic instrument. The vitreous chamber of one eye was injected with CTb conjugated to Alexa Fluor 488 (item C-22841; Molecular Probes, Eugene, OR), and the other eye was injected with CTb conjugated to Alexa Fluor 594 (item C-22842; Molecular Probes). Injections were made with a Hamilton syringe and a slightly blunted needle. Initially, injected concentrations of the two fluorescent tracers were the same [25 μg/5 μl 2% dimethylsulfoxide (DMSO) in 0.9% saline vehicle]. However, the CTb/Alexa Fluor 488 conjugate has lower specific activity (5.8 moles of dye compared with 7.0 moles for the CTb/Alex Fluor 594 conjugate) and was not as visually robust (N = 2 cut horizontally; N = 14 cut coronally, 4 with colchicine treatment). Therefore, the concentration of the CTb/Alexa Fluor 488 was increased to 33.3 μg/5 μl 7% DMSO in saline vehicle (N = 5 cut coronally; N = 6 cut horizontally, 2 with colchicine treatment). This provided a number of moles approximately equivalent to those for the other tracer and the subjective impressions of the transported tracers were similar. Three days after tracer injection, hamsters were deeply anesthetized with pentobarbital as before and transcardially perfused with 0.9% saline, followed by 4% paraformaldehyde in phosphate buffer (0.1 M, pH 7.4). The brains were removed and postfixed in the formalin solution for 2–3 hours, left to sink in 20% sucrose for 2 days, then sectioned in the coronal or horizontal plane at 30 μm on a freezing-stage sliding-block microtome. For most brains, four tissue series were collected in 0.01 M phosphate-buffered saline (PBS; pH 7.2, with 0.05% sodium azide added). For two brains, a single complete series through the SCN was collected. The sections were mounted on gelatin-subbed slides, air dried, and coverslipped using Krystalon (Diagnostic Systems, Inc., Gibbstown, NJ).

Neurons that are darkly immunoreactive for γ-aminobutyric acid (GABA) delineate the hamster SCN, but require pretreatment with colchicine for proper visualization (Morin and Blanchard, 2001). Thus, to examine the relationship between retinal ganglion cell projections and GABA neurons in the SCN, a separate set of animals (N = 4) was administered intraocular tracer injections as described above. After 3 days for tracer transport, each animal was again deeply anesthetized with pentobarbital (as described above) and placed in a stereotaxic instrument. The skull was surgically exposed, cleaned and an opening drilled to permit stereotaxic placement of a needle

attached to a 5 μl Hamilton syringe into the third ventricle on the midline, 0.4 mm rostral to bregma and 7.5 mm below the dura. A 10 μl volume of colchicine solution (1 mg colchicine/50 μl 0.9% saline) was injected over a period of 10 minutes. Twenty-four to thirty-six hours later, each animal was anesthetized, perfused, and the brains prepared and cut as described above. Procedures involving live animals were approved by the institutional animal care and use committee at Stony Brook University, where the work was performed.

Immunohistochemical reactions for GABA, calbindin-D_{28K} (Calb), and neuropeptide Y (NPY) were performed on free-floating sections. A series of sections from each brain treated with colchicine was incubated with anti-GABA primary antibody (guinea pig antiserum; Protos Biotech Corp., New York, NY; dilution 1:250) at 4°C for 36–72 hours. A separate series of sections was incubated with the anti-Calb primary antibody (rabbit antiserum; Chemicon, Temecula, CA; dilution 1:50) at 4°C for 36–72 hours. A third tissue series was incubated with anti-NPY primary antibody (rabbit antiserum; Peninsula Laboratories, San Carlos, CA; dilution 1:500) for 36–72 hours. Immunoreactivities to GABA, Calb, and NPY were visualized using the fluorescent streptavidin conjugate Alexa 647 (Molecular Probes). The sections were then mounted on gelatin-subbed slides and coverslipped as described above. Fluorescent light microscopy and digital photography were accomplished with a Zeiss Axioplan II microscope and Axiocam. Confocal laser scanning images were obtained with a Nikon E800 microscope and a Bio-Rad Radiance 2000 system. No attempt was made to determine whether individual cells received innervation from each retina. All images are digital and have a depth of field of about 0.98, 0.61 and 0.28 μm for the 20× and 40× or 60× objectives, respectively. The images have been modified only to adjust contrast and brightness. Reference was also made to a library of coronal or horizontal sections showing retinal projections in the normal hamster brain as traced by anterograde transport of CTb and subsequent CTb-immunoreactivity (-IR). Much of the information in that library has been previously reported (Morin and Blanchard, 1997, 1999).

A semiquantitative method was used to evaluate the density of ipsi- and contralateral retinal projections to regions of the SCN in four animals with bilaterally robust intraocular tracer injections. TIFF files of monochromatic, false-color images obtained with the confocal microscope and a 20× objective were imported to Corel Photo-Paint 9. The files for each color were initially modified, using the "Image→Adjust→Auto Equalize" command, which redistributed the pixel values across the entire tonal range of each image. This was followed by selecting the "Image→Transform→Threshold" and enabling the "Bi-level" threshold feature. The "High-level" slider was set equal to the rightmost bar on the histogram; "Low-level" remained at zero; "Threshold" was set to 50% of the "High-level" value. This step eliminated the color and provided an initial threshold adjustment distinguishing signal from background. Each transformed file was then converted to eight-bit gray scale and retransformed according to the above-mentioned steps, but with "Threshold" reset equal to one less than the "Threshold" value determined in the above-mentioned steps (other features unchanged). This created an image with black background and white foreground. The modified file was saved, then imported into the image-analysis program, ImageJ (http://rsb.info.nih.gov/ij), in which the black background pixels were counted in a specific region and subtracted from the total pixels in that region in order to obtain the count of foreground white pixels identifying structures containing tracer (see Fig. 1). The round, central template was created to include the region of Calb-IR neurons. A similar procedure was applied to the leaflet portion of the IGL. The semiquantitative methods are modifications of procedures previously employed (Huberman et al., 2002). The validity of the method was established by counting the total foreground pixels (N = 4) identified by CTb-Alexa 564 in the one SCN following tracer injection into the eye contralateral to it and comparing those numbers with the counts obtained in the other SCN following injection of the other eye with CTb-Alexa 488. The counts did not differ statistically.

RESULTS

Sensitivity of the tracers

In general, the CTb-Alexa fluorophore conjugates employed in this study were nearly as effective as CTb immunoreactivity visualized using the ABC method with diaminobenzidine (DAB) as the chromogen and darkfield microscopy (see Discussion). Retinal projections were visible in all nuclei of the subcortical visual shell. In the hypothalamus, the densest retinal projection is to the suprachiasmatic nucleus, with additional sites including the anterior, dorsomedial, lateral nuclei; the subparaventricular region; and the ventrolateral preoptic area. Projections extending to the piriform cortex are also visible. Contralateral terminal fields are generally denser than ipsilateral fields, and, in some regions, the ipsilateral projections are quite sparse, e.g., the lateral posterior nucleus. Nevertheless, the ipsilateral input to these regions is visible. In some brain regions, however, the tracer was not reliably seen. The sparse retinal projections to the anterior amygdaloid area, lateral piriform cortex, and more rostral areas observable in tissue prepared with peroxidase ABC methods (Morin and Blanchard, 1999) are reduced or not evident at all in brains of hamsters injected with the CTb/Alexa fluorescent tracers. In addition, the ipsilateral projection to the bed nucleus of the stria terminalis could not be seen with CTb/fluorescent conjugate as the tracer. Table 1 provides a summary of the results.

Hypothalamus and basal forebrain

The retinohypothalamic tract (RHT) of each retina projects to virtually the entire SCN (Fig. 1). However, the density of retinal innervation within the SCN varies according to region. In particular, retinal innervation of the medial SCN is less than that in most other areas in the nucleus. Moreover, the projections from the two eyes are asymmetrically distributed within the SCN. An obvious asymmetry occurs in the ventral and medial region that receives a predominantly ipsilateral projection (Fig. 1). A second asymmetry is located more laterally and dorsally. Projections to this region are dense and predominantly from the contralateral retina. Nevertheless, both retinas project to each area. The region receiving the dense contralateral projection encompasses the central subnucleus of the SCN, here identified by the presence Calb-IR neurons (Fig. 2A–C). Not only is the subnucleus infiltrated by retinal projections predominantly from the contralateral

TABLE 1. Density of the Terminal Fields Relative to the Retina of Origin Estimated From the Visual Projections Traced With Fluorescently Tagged CTb[1]

	Retina of origin	
	Ipsilateral	Contralateral
Hypothalamus		
DMH	Sparse	Sparse
LH	V. sparse	Sparse
SCN	Moderate	Dense
sPVz	Modest	Modest
Basal forebrain		
BNSTPM	V. sparse[2]	Moderate
NDB	V. sparse	Sparse
PIR	V. sparse	V. sparse
VLPO	V. sparse	Sparse
Thalamus		
IGL	Modest	Moderate
VLG	Variable	Dense
Pretectum		
APT	V. sparse	Sparse
CPT	V. sparse	Sparse
MPT	Sparse	Dense
NOT	V. sparse	Dense
OPT	Variable	Dense
PLi	Sparse	Moderate
PPT	Variable	Dense

[1]Ratings of innervation density: dense, moderate, modest, sparse, very sparse, none.
[2]A sparse ipsilateral projection was observed in tissue reacted for CTb-IR by using ABC methods, although none was visible with the fluorescent methods.

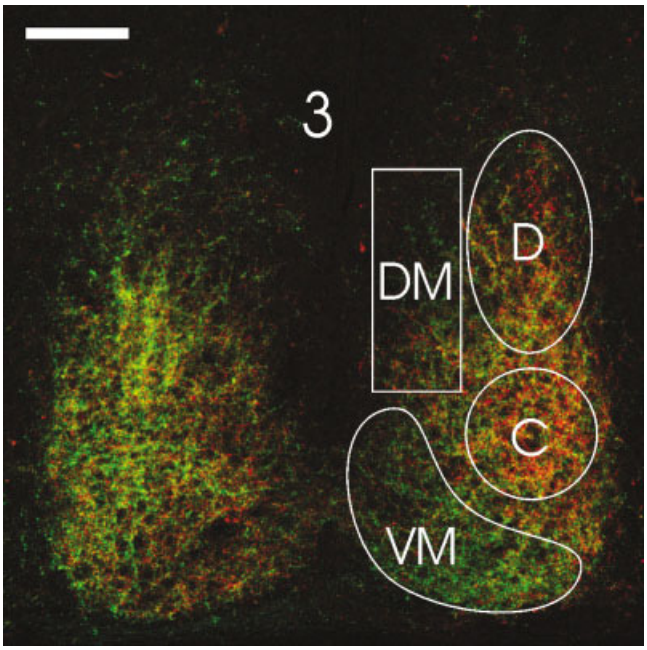

Fig. 1. Confocal laser scanning microscopic image of an optical section in the coronal plane through the central portion of the paired SCN. The animal was injected intraocularly with CTb/Alexa 488 conjugate in one eye and CTb/Alexa 594 in the other. The terminal fields of the RHT are visible as green pseudocolor or red pseudocolor representing the two tracers, respectively. The white outlines indicate the templates used to calculate label abundance in specific regions of the SCN. The densely innervated central (C) and dorsal (D) regions contain a preponderance of terminals from the contralateral retina, whereas the moderately innervated dorsomedial (DM) and ventromedial (VM) SCNs receive most of their input from the ipsilateral retina. Yellow pseudocolor is an artifact of low magnification in this and all subsequent figures. It is not true colocalization. None is expected here, and none is evident when the tissue is examined with a 63× objective (cf. Fig. 2B,C). 3, Third ventricle. Scale bar = 200 μm.

retina, but the region surrounding the central subnucleus and extending dorsal to it is also innervated predominantly by the contralateral retina (Fig. 2A). Thus, the preponderance (but by no means all) of the retinal projections to the Calb-IR cells is derived from the contralateral eye. In horizontal sections, the SCN can be recognized by its abundance of richly GABA-IR neurons (Fig. 3A). Retinal innervation revealed in horizontal sections (Fig. 3A,B) shows the same overall pattern as is evident in coronal plane sections. These sections further show that the contralateral retinal projection densely innervates an area encompassing the central subnucleus as well as the regions rostral, caudal, and lateral to it.

Semiquantitative analysis of ipsi- and contralateral retinal projections to the several SCN regions was also performed. The ipsi- and contralateral retinal projections to each region of the left SCN in each animal (N = 4) were subjected to the semiquantitative analytical method. These results were then averaged with the respective ipsi- and contralateral projections to the corresponding regions in the right SCN of the same individual, thereby correcting for any bias relating to apparent brightness of the specific tracers. Thus, four ipsilateral measures based on the average of the results for each tracer were available for each SCN region and could be compared with comparable measures for the contralateral regions. The results support the descriptive neuroanatomy and reveal regions of predominately ipsilateral, predominately contralateral, and approximately equal retinal innervation within the SCN (Table 2). Although the number of SCN examined was small, except for in the dorsomedial region, there was no overlap in the distributions of measurements for the ipsi- vs. contralateral density measurements.

The RHT also provides innervation of subparaventricular and dorsomedial hypothalamus from axons that pass through, or closely adjacent to, the SCN (data not shown). RHT terminal density is sparse to modest in these regions (e.g., subparaventricular region), and the terminal fields from each retina are interspersed and approximately equal bilaterally in these areas. The lateral hypothalamus receives sparse retinal projections, predominantly from the contralateral eye. Nevertheless, very sparse ipsilateral input is visible and overlaps with that from the contralateral retina.

Axons extending rostrally from the contralateral retina provide a sparse terminal field into the ventrolateral preoptic area (data not shown), retaining a position ventral to the medial part of the horizontal limb of the nucleus of the diagonal band of Broca. The terminal field spreads laterally into the ventral amygdala and piriform cortex. Ipsilateral projections to this region are present, but are very sparse. There is also a sparse contralateral, and a sparser ipsilateral, retinal projection to a rostral region near the midline and ventral to the vertical limb of the nucleus of the diagonal band of Broca. There is a modest contralateral retinal projection to the bed nucleus of the stria terminalis, posterior medial division (BNSTPM). An ipsilateral projection to this location was not seen in sections from animals injected with the CTb/Alexa tracers. Examination of tissue reacted for CTb-IR revealed a sparse ipsilateral projection. However, whether it was to the identical site as the contralateral projection could not be confirmed.

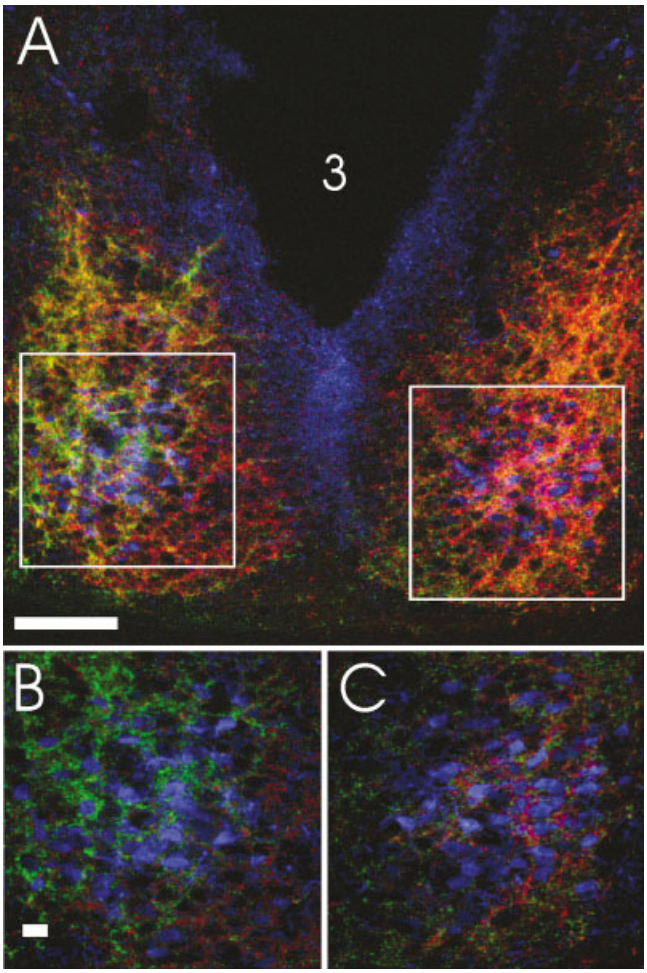

Fig. 2. **A**: Digital optical coronal section through the SCN showing the distribution of Calb-IR neurons (blue) in the central subnucleus region. Green and red pseudocolors indicate the terminal fields from the left and right retinas, respectively. The box outlines indicate the regions shown in B and C. **B,C**: High-magnification optical sections of the corresponding areas in A showing the preponderance of retinal projections to the contralateral, Calb-IR cell containing SCN subnucleus. In B, the terminal field from the contralateral retina is shown in green pseudocolor. In C, the terminal field from the contralateral retina is shown in red pseudocolor. 3, Third ventricle. Scale bar in A = 100 μm; bar in B = 10 μm for B,C.

IGL and ventral lateral geniculate nucleus

The IGL is a long, thin nucleus underlying the DLG (Fig. 4A–C) and, more caudally, the medial geniculate nucleus. Its cross-sectional outline varies substantially according to the rostrocaudal plane of section, but is fairly well defined as the sole location of NPY-IR neurons in the lateral geniculate region (Fig. 4D). Both eyes project to all levels of the IGL, but the projection from the contralateral retina is moderately dense and predominates over that of the ipsilateral retina. The ipsilateral projection is modest and fairly uniform, but is especially visible in contrast to adjacent DLG and much of the VLG which receive largely contralateral input. Semiquantitative analysis of the leaflet portion of the IGL indicates that the contralateral retina provides denser input (62% ± 2%) to the IGL than

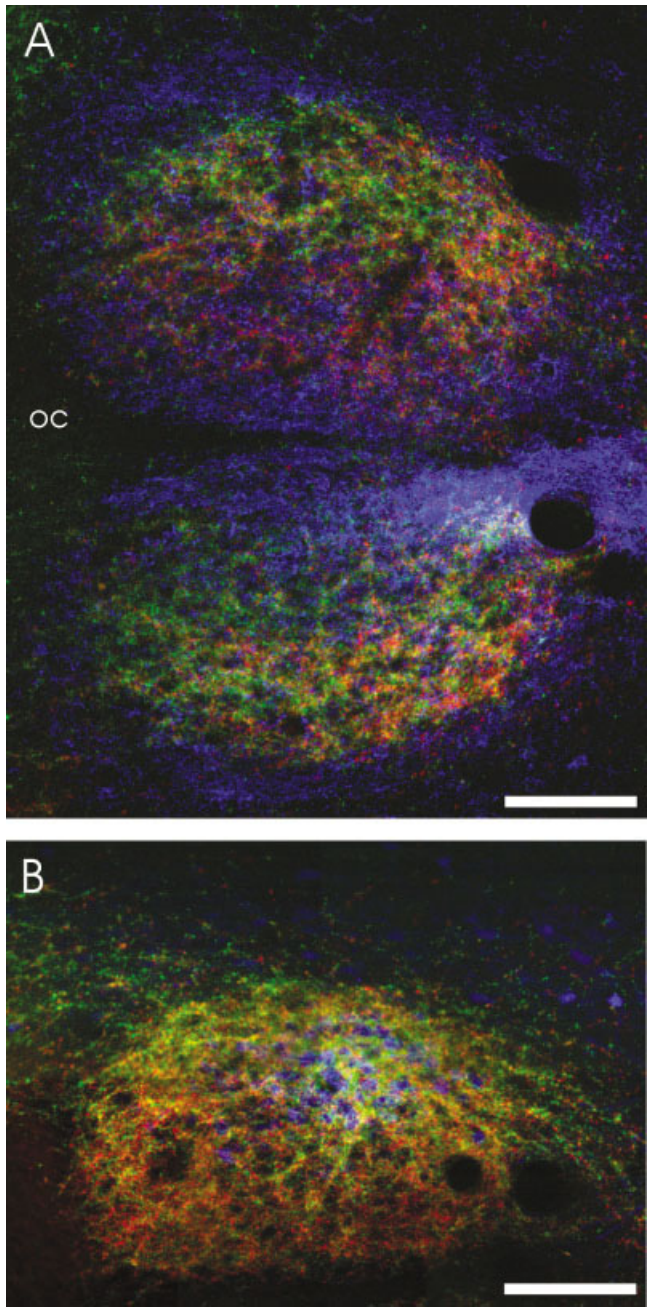

Fig. 3. Confocal laser images of optical sections through the SCN in the horizontal plane. **A**: GABA-IR neurons (blue pseudocolor cells) define each SCN. Retinal terminals are evident throughout the SCN, but the horizontal section shows clearly that the medial portion of each nucleus receives predominantly ipsilateral input (top: red pseudocolor; bottom: green pseudocolor), whereas the lateral part receives predominantly contralateral projections. **B**: Calb-IR neurons (blue pseudocolor) occupy a region in the central SCN (the image is similar in plane and orientation to the upper SCN shown in A) receiving dense input from the contralateral retina (green pseudocolor), and this is surrounded medially, rostrally, and caudally by regions in which terminals from the ipsilateral retina predominate (red pseudocolor). The plane of section is through the ventral portion of the region containing the Calb-IR cells. In A and B, rostral is to the left. Scale bars = 200 μm.

the ipsilateral retina (38% ± 2%; p = .002, t = 24.3, df = 2). Both ipsi- and contralateral retinas appear to provide fairly homogeneous innervation throughout the entire length of the IGL. The ventromedial part of the IGL, identifiable by the location of cells projecting to the SCN and peptide-containing neurons (Morin et al., 1992; Morin and Blanchard, 1998, 2001), is very sparsely innervated by each retina (lower arrows in Fig. 4A,B).

In general, the VLG is heavily innervated by the contralateral retina (Fig. 4A–C), and the densely innervated regions contain sparsely scattered projections from the ipsilateral retina. However, there are two types of exceptions to this generalization. Some regions within the VLG are less densely innervated by the contralateral retina than most of the nucleus (e.g., central VLG in Fig. 4B). In addition, some portions of the VLG are innervated almost exclusively by the ipsilateral retina. A very dense terminal field derived from the ipsilateral retina encompasses much of the dorsomedial VLG. This terminal plexus is contiguous with the overlying ventromedial IGL (Fig. 4A–C) and is a distinguishing feature indicating the dorsomedial border between the IGL and the VLG. Other, somewhat smaller patches of dense innervation from the ipsilateral retina are found elsewhere in the VLG (Fig. 4A). These contain sparsely scattered terminals from the contralateral retina, unlike the larger medial patch, which is essentially devoid of direct innervation from the contralateral retina.

TABLE 2. Semiquantitative Density (%) of Projections to Specific Regions of the SCN From Ipsi- and Contralateral Retina

	Ipsilateral retina	Contralateral retina	t (df = 3)[1]	P (two-tail)
Whole nucleus	45 ± 2	55 ± 2	3.93	<.03
Central region	37 ± 4	63 ± 8	4.72	<.02
Dorsal region	35 ± 5	65 ± 6	5.54	<.02
Dorsomedial region	49 ± 6	51 ± 7	0.33	NS
Ventromedial region	71 ± 13	29 ± 7	−3.93	<.03

[1]t-Test for dependent measures.

Pretectum

Most of the retinal input to the pretectum arrives from the contralateral retina. The bulbous, dorsal part of the PLi receives a moderately dense contralateral retinal projection (Fig. 5A) that is overlapped by a sparse terminal field from the ipsilateral retina. The vertically oriented, laminar part of the PLi is delineated by a modest terminal plexus derived from the contralateral retina that is overlapped by a sparse projection from the ipsilateral retina. Dorsomedial to the PLi, the NOT has a dense terminal

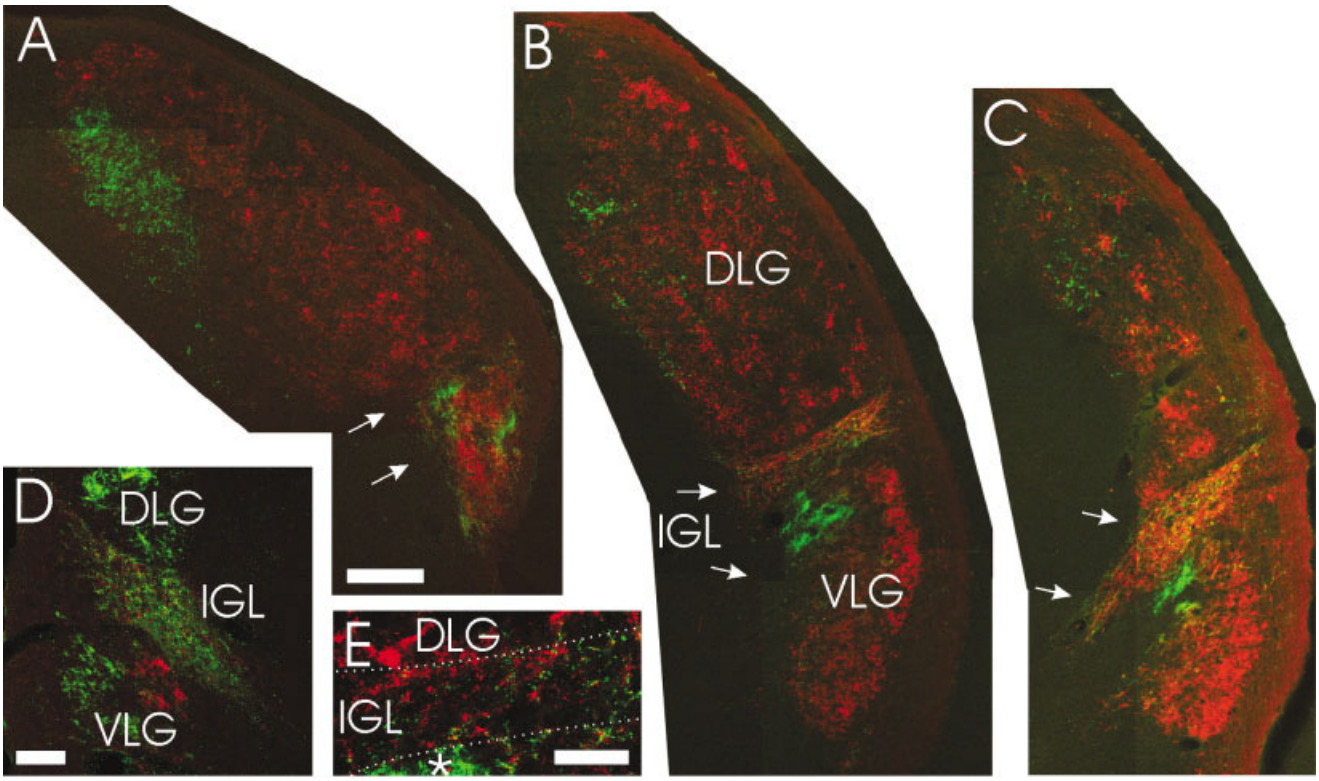

Fig. 4. Composite, coronal plane, confocal microscopic views showing ipsilateral (green pseudocolor) and contralateral (red pseudocolor) retinal projections to nuclei of the lateral geniculate complex at rostral (**A**), middle (**B**), and caudal (**C**) levels. Arrows indicate the medial border of the IGL. **D**: The IGL is shown at a level slightly caudal and contralateral to the image shown in C, with contralateral (green pseudocolor) retinal projections evident in the ventral DLG, IGL, and VLG. Ipsilateral retinal projections are shown as red pseudocolor. **E**: High-magnification image of a portion of the IGL at a level approximately equal to that in B showing the predominantly contralateral input (red pseudocolor) interspersed with terminals from the ipsilateral (green pseudocolor) retina. The asterisk indicates dense ipsilateral innervation of the dorsomedial VLG. Scale bar in A = 200 μm for A–C; bar in D = 100 μm; bar in E = 50 μm.

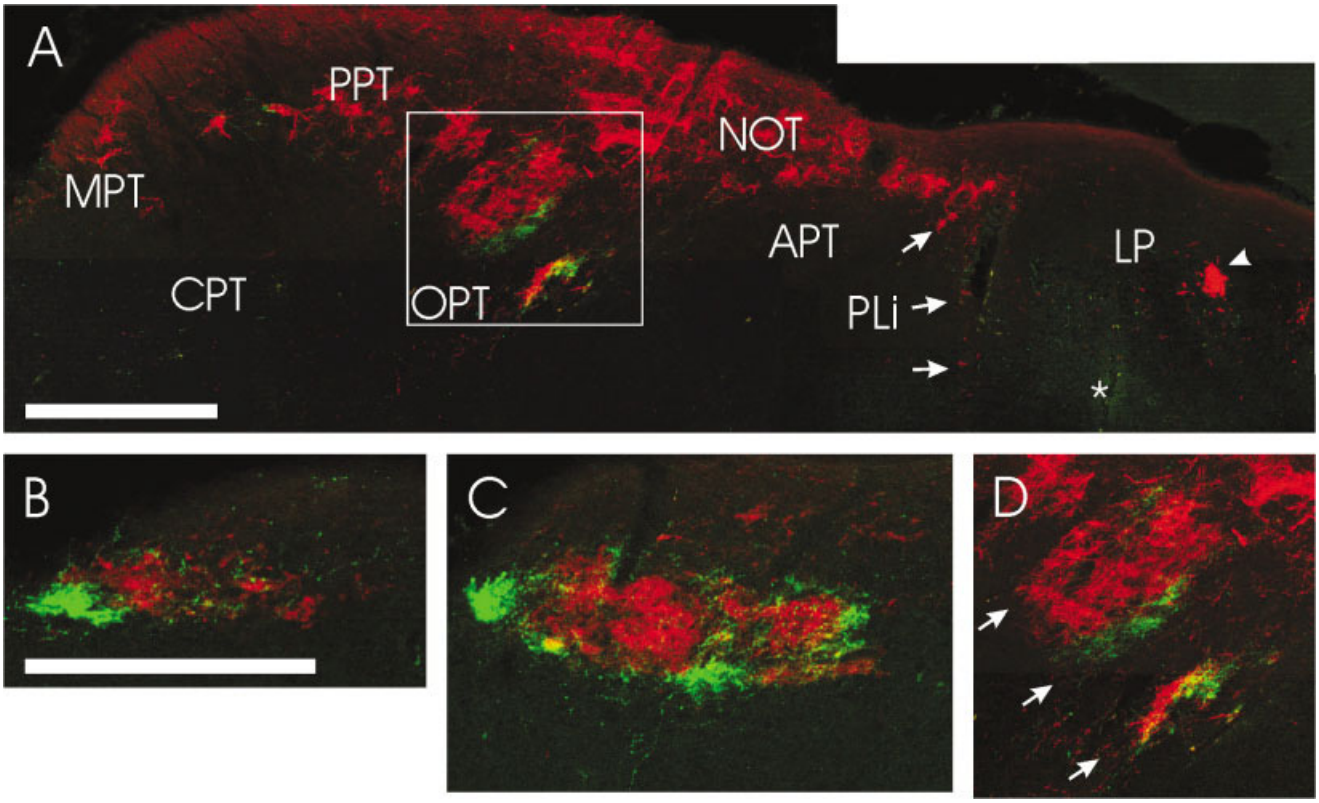

Fig. 5. **A**: Composite, coronal plane, confocal microscopic view showing largely contralateral retinal projections (red pseudocolor) to nuclei in the pretectum and thalamic lateral posterior nucleus; the ipsilateral retinal projections are shown in green pseudocolor. The arrowhead indicates a patch of dense LP terminal field from the contralateral retina. The arrows indicate the sparsely innervated laminar portion of the PLi ventral to the more densely innervated, bulbous part. Asterisk, area of green artifact. The boxed area is enlarged in D. **B–D**: Coronal views of ipsi- and contralateral retinal innervation in the OPT at three rostral to caudal levels. B is a section through the rostral part of the nonlaminar portion of the OPT. C is a section through the caudal part of the nonlaminar portion of the OPT. Arrows in D point to the three laminae of the OPT, the dorsal and ventral of which receive retinal projections and are separated by a lamination with little to no retinal input. The midline is at the left border of A. APT, anterior pretectal nucleus; CPT, commissural pretectal nucleus; LP, lateral posterior nucleus; MPT, medial pretectal nucleus; NOT, nucleus of the optic tract; PLi, posterior limitans nucleus; PPT, posterior pretectal nucleus. Scale bar in A = 500 μm; bar in B = 500 μm for B–D.

plexus from the contralateral retina, but has only very sparse innervation from the ipsilateral retina.

The dorsal division of the APT receives very sparse to sparse, coextensive innervation from both retinas (Fig. 5A). It is less visible with the present CTb/Alexa fluorophore conjugates than with CTb immunohistochemistry (Morin and Blanchard, 1997). The contralateral projection to the APT is slightly denser than the ipsilateral projection.

Retinal projections, on which descriptions of the OPT are based (Scalia and Arango, 1979), innervate an elliptically shaped rostromedial "head" region (Fig. 5B,C) that becomes laminar (Fig. 5A,D) as it angles caudolaterally away from the midline. Two of the laminae consist of a thicker dorsomedial layer and a ventrolateral layer, both of which are densely retinorecipient. These are separated by the third lamina, which has sparse retinal innervation, but which receives projections containing NPY-IR (Morin and Blanchard, 1997). The OPT receives dense innervation from the contralateral retina. However, a few subregions of the nucleus have obvious terminal plexuses derived solely from the ipsilateral retina. There are also portions of the OPT in which there is overlap of the terminal fields from each retina. Rostrally, one ipsilateral contribution is evident at the medial aspect of the OPT (Fig. 5B), and it persists caudally along the elliptical "head" of the nucleus (Fig. 5C). At the transition to the laminar part of the nucleus, dense terminal fields from the ipsilateral retina are evident ventrally and laterally (Fig. 5C). In the laminar part of the OPT, the bulk of the dorsomedial lamination receives a projection from the contralateral retina, but a projection from the ipsilateral retina is evident along its ventrolateral surface (Fig. 5D). The thinner ventrolateral lamination also has a region containing dense terminals from the ipsilateral retina, as well as a clear zone of overlap with interspersed terminals from each retina (Fig. 5D).

The MPT and portions of the PPT receive dense input almost exclusively from the contralateral retina (Fig. 5A). In the PPT, there are small regions of exclusively ipsilateral innervation plus areas of interspersed terminals from each retina. Ipsilateral retinal projections are sparse in the MPT and interspersed among those from the contralateral retina. The CPT receives sparse projections from the contralateral retina, whereas the ipsilateral projection to the same region is very sparse.

DISCUSSION

The function of the SCN circadian clock is influenced by the activity of the IGL (for review see Morin, 1994) and visual midbrain (Marchant and Morin, 1999). The SCN, IGL and pretectum (the OPT, in particular) share an additional characteristic to the extent that all three receive dense projections from photoreceptive melanopsin-containing retinal ganglion cells (Provencio et al., 1998; Gooley et al., 2001; Hannibal et al., 2002; Hattar et al., 2002; Morin et al., 2003; Gooley and Saper, 2003). The present results show three different patterns of retinal innervation to these areas. In the OPT, ipsi- and contralateral retinal terminal fields are largely nonoverlapping, whereas they are completely overlapping in the IGL and SCN. However, the pattern of overlap in the IGL differs substantially from that in the SCN. In the IGL, the innervation is predominantly from the contralateral retina, with both eyes providing homogeneous terminal fields. In the SCN, the terminal fields from each retina encompass the entire SCN, but there are regions in which either the ipsi- or the contralateral projections predominate.

Technical considerations

We have previously identified hamster retinorecipient regions employing the sensitive tracer CTb and immunohistochemistry with DAB as the chromogen. Those studies revealed widespread retinal projections throughout the pretectal nuclei, including the posterior limitans and the commissural pretectal area to which visual projections had not previously been reported (Morin and Blanchard, 1997). The present approach employed CTb conjugated to one of two fluorescent labels, Alexa 488 or Alexa 594. These provide brilliant signals and, given that each CTb conjugate was present in all retinorecipient regions previously documented by CTb-IR, the use of the CTb/Alexa conjugates appears to have a level of sensitivity very similar to that found with immunohistochemistry and dark-field microscopy. However, innervation of some regions, such as the piriform cortex, anterior amygdala and inferior colliculus, which appears to be sparse when evaluated with ABC methods, seems even sparser with the current fluorescent tracer procedures. The location with the clearest instance of reduced visibility of the fluorescent tracer was the BNSTPM, in which only the contralateral projection could be seen, although visualizing CTb-IR with ABC methods and DAB reveals a sparse ipsilateral projection as well.

It should be noted that the signal strength of Alexa 488 appeared to be less than that for Alexa 594. Subjective estimates of relative innervation density can be complicated. For locations such as the DLG that receive very dense contralateral and ipsilateral projections with essentially no overlap, estimates of this type are obvious. However, where the extent of innervation from each retina is fairly sparse, but dissimilar, judgments are more difficult. Moreover, in the present study, innervation density is related to the perceived intensities of red and green, each a pseudocolor applied by computer software to the digital images obtained from analysis of fluorophore intensity. Judgments of innervation density were improved by raising the concentration of CTb/Alexa 488 conjugate injected intraocularly. This method provided an acceptable qualitative and quantitative (data not shown) balance of apparent red and green pseudocolors during simultaneous evaluation of projections to the ipsi- and contralateral SCN.

Retinohypothalamic tract

Previous investigations employed unilateral eye injections to identify retinohypothalamic tract projections to the hamster SCN. Studies with fairly sensitive tracing methods, such as HRP or cholera toxin-HRP, have shown that much, if not all, of the nucleus receives input from each retina (Pickard and Silverman, 1981; Youngstrom and Nunez, 1986; Johnson et al., 1988b). Autoradiographic methods substantially underestimate retinal innervation of the hamster SCN (Eichler and Moore, 1974; Card and Moore, 1984).

The present results show that, across the entire SCN, about 55% of the innervation is derived from the contralateral retina. This is consistent with the earlier studies indicating that about 50% of the terminals from each retina are present in each hamster SCN. However, the present data also provide the first demonstration of substantial asymmetry within the SCN with respect to retinal terminal field density. Previous studies suggested that the ipsi- and contralateral projections were similarly distributed throughout the hamster SCN (Eichler and Moore, 1974; Pickard and Silverman, 1981; Johnson et al., 1988b). Asymmetries were probably overlooked for two major reasons: tissue section thickness and an inability to compare directly locations of projections from each retina in the same section. The combined use of confocal laser scanning microscopy and dual fluorescent tracers has essentially eliminated these problems.

The SCN is widely recognized as the locus of the principal circadian clock of the brain (Klein et al., 1991). Rhythms generated in, and hierarchically driven by, the SCN are entrained to the ambient photoperiod via the retinohypothalamic tract (Rusak, 1977; Johnson et al., 1988a). In rodents, retinal ganglion cells projecting to the SCN are located throughout all four quadrants of both retinas in relatively equal densities regardless of whether they project ipsi- or contralaterally (Pickard, 1980, 1982; Morin et al., 2003). Comparative anatomical investigation of the retinohypothalamic projection to the SCN has demonstrated that asymmetry of the ipsi- and contralateral projections is widespread among mammals (Moore, 1973; Johnson et al., 1988b; Magnin et al., 1989; Cooper et al., 1993). In most species, the asymmetry consists of the contralateral projection being clearly denser than the ipsilateral projection. In the hamster, approximately 55% of ganglion cells projecting to one SCN reside in the contralateral retina (Pickard, 1982; Morin et al., 2003). Function of the differing ipsi- and contralateral retinal projections has not been established, although it has been suggested that rate of circadian rhythm reentrainment may be related to the extent of putative retinohypothalamic tract symmetry (Stephan et al., 1982). In the present context, there has been no previous attention to ipsi- vs contralateral differences of retinal projection distribution within a single SCN of any species. The fact that individual retinal ganglion cells bifurcate and project to each SCN (Morin et al., 2003) further complicates understanding of RHT terminal field patterning within each nucleus.

The hamster SCN contains a distinct central subdivision characterized by specific cell types, including those containing substance P (Morin et al., 1992), gastrin-

releasing peptide (Aioun et al., 1998), calretinin (Blanchard and Morin, unpublished data), and Calb (Silver et al., 1996). Nocturnal light induces FOS protein expression in about 80% of the Calb-IR cells (Silver et al., 1996), and the Calb-IR cells in this region receive retinal innervation in the form of axosomatic synapses (Bryant et al., 2000). The Calb neurons may be a necessary part of the photoentrainment pathway (LeSauter and Silver, 1999). However, analysis of light-induced FOS or the clock-related genes Per1 and BMAL in SCN neurons (Guido et al., 1999; Hamada et al., 2002) suggests substantially greater retinal innervation of the SCN than simply to the area containing Calb-IR cells. The present data show that the region of Calb-IR neurons receives input from both retinas, with the contralateral projection considerably denser than that from the ipsilateral eye. The dense contralateral terminal field, although clearly encompassing the Calb neurons, also extends well dorsal to them. This result is consistent with the demonstration that the region of light-induced FOS or clock-related proteins also encompasses, but extends beyond, the central SCN area (Guido et al., 1999; Hamada et al., 2002). The dense contralateral terminal field also appears to provide a fairly close match to the region containing the nocturnally phosphorylated, and retina-dependent, mitogen-activated protein kinases ERK1 and ERK2 (Lee et al., 2003).

The specialized central region of the hamster SCN is surrounded by a dorsomedial zone containing vasopressin and cholecystokinin cells and a ventral region containing neurons immunoreactive to vasoactive intestinal polypeptide (Card and Moore, 1984; LeSauter et al., 2002). This area approximates the combined dorsomedial and ventromedial regions shown here to receive predominantly ipsilateral innervation. It also corresponds to the area of dense serotonergic innervation from the median raphe nucleus (Meyer-Bernstein and Morin, 1996). This suggests the possibility that the inhibitory, presynaptic effects of serotonin on light-induced circadian rhythm responses (Morin and Blanchard, 1991; Meyer-Bernstein and Morin, 1996; Pickard et al., 1999) might be mediated through the ipsilateral projections to the regionally associated classes of peptidergic neurons.

Elsewhere in the hypothalamus, retinal innervation is considerably less than that in the SCN, although the preponderance of retinal input is from the contralateral eye (Table 1). Unlike the case for the SCN, there do not appear to be any regions in which the ipsilateral projection predominates. Despite the fact that the RHT is widely known to project to several hypothalamic nuclei other than the SCN, there is no known visual function for any of them. One possibility is "masking" of circadian locomotor activity. Negative masking (decreased activity) is a well-documented response to light (Mrosovsky, 1999). Lesions of the IGL, DLG, or visual cortex actually enhance negative masking by light, but no retinorecipient region has yet been identified as necessary for light-induced negative masking, including the SCN (Redlin and Mrosovsky, 1999; Redlin et al., 1999, 2003; Edelstein and Mrosovsky, 2001).

More rostrally, innervation of the lateral preoptic area is well established (Johnson et al., 1988b; Lu et al., 1999). The present data affirm that the ventrolateral preoptic area receives direct retinal input, predominantly from the contralateral retina, a region that, in the rat, also receives sparse afferents from the SCN (Chou et al., 2002). This region has long been considered a mediator of sleep, with lesions producing insomnia (Nauta, 1946; Lu et al., 2000). The nucleus of the diagonal band of Broca and piriform cortex in nearby basal forebrain also receive sparse and predominantly contralateral retinal input (Table 1). The function of this innervation has not been established. Similarly, there is a moderate retinal projection to the contralateral BNSTPM (the ipsilateral projection is very sparse and is visible only with ABC methods to evaluate CTb-IR). A visual function for this region has not been identified, although it might mediate light-facilitated acoustic startle (Walker and Davis, 1997). The baseline acoustic startle response itself has clear circadian rhythm modulation (Chabot and Taylor, 1992; Frankland and Ralph, 1995), and entrainment of this rhythm is likely to be via the RHT and separate from the visual circuitry by which acoustic startle is light facilitated.

IGL

The IGL has a well-documented role as one of the nuclei of the "circadian visual system" (Morin, 1994). The IGL contributes to circadian rhythm regulation by both photic (Harrington and Rusak, 1986; Pickard et al., 1987; Johnson et al., 1989; Morin and Pace, 2002) and nonphotic (Mrosovsky, 1996; Turek and Losee-Olson, 1986; Reebs and Mrosovsky, 1989) stimuli. The IGL receives direct retinal input (Hickey and Spear, 1976; Pickard, 1982; Morin et al., 1992; Moore and Card, 1994; Morin and Blanchard, 1997; Ling et al., 1998; present results). Both photic and nonphotic effects of IGL-mediated phase shifts on circadian rhythmicity are presumed to occur via NPY projections in the geniculohypothalamic tract to the SCN from the IGL (Albers et al., 1984; Johnson et al., 1988c; Card and Moore, 1989; Biello et al., 1994; Wickland and Turek, 1994; Morin and Blanchard, 2001).

Fewer ipsi- than contralateral retinal ganglion cells project to the IGL (Blanchard et al., 2002), but the contralateral projection density is only modestly greater (present data). Both eyes provide retinal terminal fields in the IGL that are completely interspersed and that encompass the entire nucleus (present data; Morin et al., 1992). How these characteristics of terminal overlap and distribution in the IGL contribute to circadian rhythm regulation or other visual function (e.g., Legg, 1975) is not known.

It is still uncertain whether the IGL has a noncircadian visual function, although recent anatomical literature suggests that this may be the case (Shiroyama et al., 1999). In addition to having reciprocal, usually bilateral, connections with nearly all the major subcortical retinorecipient nuclei, the IGL has connections with numerous nonretinorecipient structures as well (Morin and Blanchard, 1998, 1999; Moore et al., 2000). Circadian rhythm regulation can be modified by pretectal or tectal lesions or by severing the connections between the IGL and those areas; electrical stimulation of the sensory midbrain can stimulate phase shifts of the circadian clock during the subjective day and greatly reduce phase shifts in response to light during the subjective night (Marchant and Morin, 1999). This growing amount of evidence suggests that information from multiple sensory modalities may converge upon the IGL, modulating output of the SCN via the geniculohypothalamic tract.

The dorsomedial VLG also has a dense terminal field arising exclusively from the ipsilateral retina. This region is fairly long, extending about half the 2-mm length of the

IGL, and is distinguished from the IGL by the absence of NPY-IR neurons and cells that project to the SCN (present data; Morin et al., 1992; Morin and Blanchard, 2001).

Pretectum

The visual midbrain contributes to the regulation of hamster circadian rhythmicity, although it is not clear whether the site is in the pretectum or tectum (Marchant and Morin, 1999). The most intensively studied pretectal region is the olivary pretectal nucleus, best known for its contribution to the consensual pupillary light reflex (Clarke and Ikeda, 1985; Klooster et al., 1995; Young and Lund, 1997). The topographic organization of bilateral retinal projections to the OPT is more diverse than that of the other regions described here. Some regions receive projections exclusively from one retina or the other; others receive approximately equal ipsi- and contralateral input. Elsewhere in the pretectum, ipsilateral retinal innervation is generally sparse. The contralateral input to these nuclei is uniformly greater than that from the ipsilateral retina, although the density of the contralateral projection varies substantially across nuclei (Table 1), which is consistent with our previous observations (Morin and Blanchard, 1997).

Projections of melanopsin-containing ganglion cells

The presence of interspersed retinal input to the SCN and IGL could be related to the fact that each nucleus receives input from a novel class of photoreceptive ganglion cells containing the putative photopigment, melanopsin (Gooley et al., 2001; Hannibal et al., 2002; Berson et al., 2002; Hattar et al., 2002; Morin et al., 2003). It remains to be seen whether there is regional specificity within the SCN or IGL with respect to the terminal fields of melanopsin-containing retinal ganglion cells. Melanopsin-containing ganglion cells also project to other brain regions. Those currently identified are subparaventricular hypothalamus, ventrolateral preoptic area, and SC (Morin et al., 2003; Gooley and Saper, 2003). The projections to the SCN, IGL, and OPT are substantial (Hattar et al., 2002), and their ganglion cells of origin appear to be designed for transmitting information about light intensity to the brain (Berson et al., 2002). Circadian rhythm response to light and the consensual pupillary light reflex are substantially reduced in melanopsin gene knockout mice (Panda et al., 2002; Ruby et al., 2002; Lucas et al., 2003). Photic information arriving at the SCN and IGL may be more useful to the organism if it arrives in a bilaterally redundant fashion, i.e., with overlapping terminal fields from each retina. The OPT appears to have a specific role in controlling bilateral symmetry of light-induced pupillary constriction that may be more easily managed when inputs from each retina target different populations of midbrain neurons.

In summary, we have injected different fluorescent tracers into each eye and evaluated the contribution of ipsi- and contralateral retinal projections to retinorecipient regions implicated in the regulation of circadian rhythmicity. The results demonstrate different patterns of innervation evident in the three brain nuclei, the SCN, IGL, and OPT, examined in detail. Although the contralateral retina generally provides the preponderance of innervation to each of these nuclei, there are specific regions in the SCN and OPT where the ipsilateral projection predominates partially (SCN) or exclusively (OPT). Circadian rhythm function of the ipsi- and contralaterally derived retinal terminal fields is not known.

ACKNOWLEDGMENTS

We are very grateful to Dr. Irving Zucker for his good sense, provision of fertile ground for the germination of this study, and helpful criticism of its product. Jane Blanchard and Laura Pace provided excellent technical assistance.

LITERATURE CITED

Agarwala S, Petry HM, May JG. 1989. Retinal projections in the ground squirrel (*Citellus tridecemlineatus*). Vis Neurosci 3:537–549.

Aioun J, Chambille I, Peytevin J, Martinet L. 1998. Neurons containing gastrin-releasing peptide and vasoactive intestinal polypeptide are involved in the reception of the photic signal in the suprachiasmatic nucleus of the Syrian hamster: an immunocytochemical ultrastructural study. Cell Tissue Res 291:239–253.

Albers HE, Ferris CF, Leeman SE, Goldman BD. 1984. Avian pancreatic polypeptide phase shifts hamster circadian rhythms when microinjected into the suprachiasmatic region. Science 223:833–835.

Berson DM, Dunn FA, Takao M. 2002. Phototransduction by retinal ganglion cells that set the circadian clock. Science 295:1070–1073.

Biello SM, Janik D, Mrosovsky N. 1994. Neuropeptide Y and behaviorally induced phase shifts. Neuroscience 62:273–279.

Blanchard JH, Provencio I, Morin LP. 2002. Innervation of hamster visual system by melanopsin-containing retinal ganglion cells. Soc Neurosci, 32 Abstr 371.4.

Bryant DN, LeSauter J, Silver R, Romero MT. 2000. Retinal innervation of calbindin-D28K cells in the hamster suprachiasmatic nucleus: ultrastructural characterization. J Biol Rhythms 15:103–111.

Card JP, Moore RY. 1982. Ventral lateral geniculate nucleus efferents to the rat suprachiasmatic nucleus exhibit avian pancreatic polypeptide-like immunoreactivity. J Comp Neurol 206:390–396.

Card JP, Moore RY. 1984. The suprachiasmatic nucleus of the golden hamster: immunohistochemical analysis of cell and fiber distribution. Neuroscience 13:390–396.

Card JP, Moore RY. 1989. Organization of lateral geniculate-hypothalamic connections in the rat. J Comp Neurol 284:135–147.

Chabot CC, Taylor DH. 1992. Daily rhythmicity of the rat acoustic startle response. Physiol Behav 51:885–889.

Chou TC, Bjorkum AA, Gaus SE, Lu J, Scammell TE, Saper CB. 2002. Afferents to the ventrolateral preoptic nucleus. J Neurosci 22:977–990.

Clarke RJ, Ikeda H. 1985. Luminance and darkness detectors in the olivary and posterior pretectal nuclei and their relationship to the pupillary light reflex in the rat. I. Studies with steady luminance levels. Exp Brain Res 57:224–232.

Cooper HM, Herbin M, Nevo E. 1993. Visual system of a naturally microphthalmic mammal: the blind mole rat, *Spalax ehrenbergi*. J Comp Neurol 328:313–350.

Edelstein K, Mrosovsky N. 2001. Behavioral responses to light in mice with dorsal lateral geniculate lesions. Brain Res 918:107–112.

Eichler VB, Moore RY. 1974. The primary and accessory optic systems in the golden hamster, *Mesocricetus auratus*. Acta Anat 89:359–371.

Frankland PW, Ralph MR. 1995. Circadian modulation in the rat acoustic startle circuit. Behav Neurosci 109:43–48.

Goel N, Lee TM, Smale L. 1999. Suprachiasmatic nucleus and intergeniculate leaflet in the diurnal rodent *Octodon degus*: retinal projections and immunocytochemical characterization. Neuroscience 92:1491–1509.

Gooley JJ, Saper CB. 2003. A broad role for melanopsin in nonvisual photoreception based on neuroanatomical evidence in rats. J Neurosci 23:7093–7106.

Gooley JJ, Lu J, Chou TC, Scammell TE, Saper CB. 2001. Melanopsin in cells of origin of the retinohypothalamic tract. Nat Neurosci 4:1165.

Groos GA, Meijer JH. 1985. Effects of illumination on suprachiasmatic nucleus electrical discharge. Ann N Y Acad Sci 453:134–146.

Groos G, Mason R, Meijer J. 1983. Electrical and pharmacological properties of the suprachiasmatic nuclei. Fed Proc 42:2790–2795.

Guido ME, Goguen D, De Guido L, Robertson HA, Rusak B. 1999. Circadian and photic regulation of immediate-early gene expression in the hamster suprachiasmatic nucleus. Neuroscience 90:555–571.

Hamada T, LeSauter J, Venuti JM, Silver R. 2002. Expression of *Period* genes: rhythmic and non-rhythmic compartments of the suprachiasmatic nucleus pacemaker. J Neurosci 21:7742–7750.

Hannibal J, Hindersson P, Knudsen SM, Georg B, Fahrenkrug J. 2002. The photopigment melanopsin is exclusively present in pituitary adenylated cyclase-activating polypeptide-containing retinal ganglion cells of the retinohypothalamic tract. J Neurosci 22:RC191 (1–7).

Harrington ME, Rusak B. 1986. Lesions of the thalamic intergeniculate leaflet alter hamster circadian rhythms. J Biol Rhythms 1:309–325.

Harrington ME, Nance DM, Rusak B. 1985. Neuropeptide Y immunoreactivity in the hamster geniculo-suprachiasmatic tract. Brain Res Bull 15:465–472.

Harrington ME, Nance DM, Rusak B. 1987. Double-labeling of neuropeptide Y-immunoreactive neurons which project from the geniculate to the suprachiasmatic nuclei. Brain Res 410:275–282.

Hattar S, Liao HW, Takao M, Berson DM, Yau KW. 2002. Melanopsin-containing retinal ganglion cells: architecture, projections, and intrinsic photosensitivity. Science 295:1065–1070.

Hendrickson AE, Wagoner N, Cowan WM. 1972. An autoradiographic and electron microscopic study of retinohypothalamic connections. Z Zellforschung 135:1–26.

Hickey TL, Spear PD. 1976. Retinogeniculate projections in hooded and albino rats: an autoradiographic study. Exp Brain Res 24:523–529.

Huberman AD, Stellwagen D, Chapman B. 2002. Decoupling eye-specific segregation from lamination in the lateral geniculate nucleus. J Neurosci 22:9419–9429.

Johnson RF, Moore RY, Morin LP. 1988a. Loss of entrainment and anatomical plasticity after lesions of the hamster retinohypothalamic tract. Brain Res 460:297–313.

Johnson RF, Morin LP, Moore RY. 1988b. Retinohypothalamic projections in the hamster and rat demonstrated using cholera toxin. Brain Res 462:301–312.

Johnson RF, Smale L, Moore RY, Morin LP. 1988c. Lateral geniculate lesions block circadian phase shift responses to a benzodiazepine. Proc Natl Acad Sci USA 85:5301–5304.

Johnson RF, Moore RY, Morin LP. 1989. Lateral geniculate lesions alter activity rhythms in the hamster. Brain Res Bull 22:411–422.

Klein DC, Moore RY, Reppert SM. 1991. Suprachiasmatic nucleus: the mind's clock. New York: Oxford University Press.

Klooster J, Vrensen GFJM, Müller LJ, Van der Want JJL. 1995. Efferent projections of the olivary pretectal nucleus in the albino rat subserving the pupillary light reflex and related reflexes. A light microscopic tracing study. Brain Res 688:34–46.

Lee HS, Nelms JL, Nguyen M, Silver R, Lehman MN. 2003. The eye is necessary for a circadian rhythm in the suprachiasmatic nucleus. Nat Neurosci 6:111–112.

Legg CR. 1975. Effects of subcortical lesions on the pupillary light reflex in the rat. Neuropsychologia 13:373–376.

LeSauter J, Silver R. 1999. Localization of a suprachiasmatic nucleus subregion regulating locomotor rhythmicity. J Neurosci 19:5574–5585.

LeSauter J, Kriegsfeld LJ, Hon J, Silver R. 2002. Calbindin-D_{28K} cells selectively contact intra-SCN neurons. Neuroscience 111:575–585.

Ling C, Schneider GE, Jhaveri S. 1998. Target-specific morphology of retinal axon arbors in the adult hamster. Vis Neurosci 15:559–579.

Lu J, Shiromani P, Saper CB. 1999. Retinal input to the sleep-active ventrolateral preoptic nucleus in the rat. Neuroscience 93:209–214.

Lu J, Greco MA, Shiromani P, Saper CB. 2000. Effect of lesions of the ventrolateral preoptic nucleus on NREM and REM sleep. J Neurosci 20:3830–3842.

Lucas RJ, Hattar S, Takao M, Berson DM, Foster RG, Yau KW. 2003. Diminished pupillary light reflex at high irradiances in melanopsin-knockout mice. Science 299:245–247.

Magnin M, Cooper HM, Mick G. 1989. Retinohypothalamic pathway: a breach in the law of Newton-Muller-Gudden? Brain Res 488:390–397.

Marchant EG, Morin LP. 1999. The hamster circadian rhythm system includes nuclei of the subcortical visual shell. J Neurosci 19:10482–10493.

Meijer JH, Groos GA, Rusak B. 1986. Luminance coding in a circadian pacemaker: the suprachiasmatic nucleus of the rat and the hamster. Brain Res 382:109–118.

Meyer-Bernstein EL, Morin LP. 1996. Differential serotonergic innervation of the suprachiasmatic nucleus and the intergeniculate leaflet and its role in circadian rhythm modulation. J Neurosci 16:2097–2111.

Miller JD, Morin LP, Schwartz WJ, Moore RY. 1996. New insights into the mammalian circadian clock [review; 230 refs]. Sleep 19:641–667.

Moore RY. 1973. Retinohypothalamic projection in mammals: a comparative study. Brain Res 49:403–409.

Moore RY, Card JP. 1994. Intergeniculate leaflet: an anatomically and functionally distinct subdivision of the lateral geniculate complex. J Comp Neurol 344:403–430.

Moore RY, Lenn NJ. 1972. A retinohypothalamic projection in the rat. J Comp Neurol 146:1–14.

Moore RY, Weis R, Moga MM. 2000. Efferent projections of the intergeniculate leaflet and the ventral lateral geniculate nucleus in the rat. J Comp Neurol 420:398–418.

Morin LP. 1994. The circadian visual system. Brain Res Rev 67:102–127.

Morin LP, Blanchard JH. 1991. Depletion of brain serotonin by 5,7-DHT modifies hamster circadian rhythm response to light. Brain Res 566: 173–185.

Morin LP, Blanchard JH. 1995. Organization of the hamster intergeniculate leaflet: NPY and ENK projections to the suprachiasmatic nucleus, intergeniculate leaflet and posterior limitans nucleus. Vis Neurosci 12:57–67.

Morin LP, Blanchard JH. 1997. Neuropeptide Y and enkephalin immunoreactivity in retinorecipient nuclei of the hamster pretectum and thalamus. Vis Neurosci 14:765–777.

Morin LP, Blanchard JH. 1998. Interconnections among nuclei of the subcortical visual shell: the intergeniculate leaflet is a major constituent of the hamster subcortical visual system. J Comp Neurol 396:288–309.

Morin LP, Blanchard JH. 1999. Forebrain connections of the hamster intergeniculate leaflet: comparison with those of ventral lateral geniculate nucleus and retina. Vis Neurosci 16:1037–1054.

Morin LP, Blanchard JH. 2001. Neuromodulator content of hamster intergeniculate leaflet neurons and their projection to the suprachiasmatic nucleus or visual midbrain. J Comp Neurol 437:79–90.

Morin LP, Pace L. 2002. The intergeniculate leaflet, but not the visual midbrain, mediates hamster circadian rhythm response to constant light. J Biol Rhythms 17:217–226.

Morin LP, Blanchard JH, Moore RY. 1992. Intergeniculate leaflet and suprachiasmatic nucleus organization and connections in the hamster. Vis Neurosci 8:219–230.

Morin LP, Blanchard JH, Provencio I. 2003. Retinal ganglion cell projections to the hamster suprachiasmatic nucleus, intergeniculate leaflet and visual midbrain: bifurcation and melanopsin immunoreactivity. J Comp Neurol 465:401–416.

Mrosovsky N. 1996. Locomotor activity and non-photic influences on circadian clocks. Biol Rev Camb Philos Soc 71:343–372.

Mrosovsky N. 1999. Masking: history, definitions, and measurement. Chronobiol Int 16:415–429.

Muir-Robinson G, Hwang BJ, Feller MB. 2002. Retinogeniculate axons undergo eye-specific segregation in the absence of eye-specific layers. J Neurosci 22:5259–5264.

Nauta WJH. 1946. Hypothalamic regulation of sleep in rats. An experimental study. J Neurophysiol 9:285–316.

Panda S, Sato TK, Castrucci AM, Rollag MD, DeGrip WJ, Hogenesch JB, Provencio I, Kay SA. 2002. Melanopsin (Opn4) requirement for normal light-induced circadian phase shifting. Science 298:2213–2216.

Pickard GE. 1980. Morphological characteristics of retinal ganglion cells projecting to the suprachiasmatic nucleus: a horseradish peroxidase study. Brain Res 183:458–465.

Pickard GE. 1982. The afferent connections of the suprachiasmatic nucleus of the golden hamster with emphasis on the retinohypothalamic projection. J Comp Neurol 211:65–83.

Pickard GE. 1989. Entrainment of the circadian rhythm of wheelrunning activity is phase shifted by ablation of the intergeniculate leaflet. Brain Res 494:151–154.

Pickard GE, Silverman AJ. 1981. Direct retinal projections to hypothalamus, piriform cortex and accessory optic nuclei in the golden hamster as demonstrated by a sensitive anterograde horseradish peroxidase technique. J Comp Neurol 196:155–172.

Pickard GE, Ralph MR, Menaker M. 1987. The intergeniculate leaflet partially mediates effects of light on circadian rhythms. J Biol Rhythms 2:35–56.

Pickard GE, Smith BN, Belenky M, Rea MA, Dudek FE, Sollars PJ. 1999.

5-HT1B receptor-mediated presynaptic inhibition of retinal input to the suprachiasmatic nucleus. J Neurosci 19:4034–4045.

Provencio I, Jiang G, De Grip WJ, Hayes WP, Rollag MD. 1998. Melanopsin: an opsin in melanophores, brain, and eye. Proc Natl Acad Sci USA 95:340–345.

Redlin U, Mrosovsky N. 1999. Masking by light in hamsters with SCN lesions. J Comp Physiol A184:439–448.

Redlin U, Vrang N, Mrosovsky N. 1999. Enhanced masking response to light in hamsters with IGL lesions. J Comp Physiol A184:449–456.

Redlin U, Cooper HM, Mrosovsky N. 2003. Increased masking response to light after ablation of the visual cortex in mice. Brain Res 965:1–8.

Reebs SG, Mrosovsky N. 1989. Effects of induced wheel running on the circadian actvity rhythms of Syrian hamsters: entrainment and phase response curve. J Biol Rhythms 4:39–48.

Ruby NF, Brennan TJ, Xie X, Cao V, Franken P, Heller HC, O'Hara BF. 2002. Role of melanopsin in circadian responses to light. Science 298: 2211–2213.

Rusak B. 1977. The role of the suprachiasmatic nuclei in the generation of circadian rhythms in the golden hamster, *Mesocricetus auratus*. J Comp Physiol 118:145–164.

Scalia F, Arango V. 1979. Topographic organization of the projections of the retina to the pretectal region in the rat. J Comp Neurol 186:271–292.

Shiroyama T, Kayahara T, Yasui Y, Nomura J, Nakano K. 1999. Projections of the vestibular nuclei to the thalamus in the rat: a *Phaseolus vulgaris* leucoagglutinin study. J Comp Neurol 407:318–332.

Silver R, Romero MT, Besmer HR, Leak RK, Nunez JM, LeSauter J. 1996. Calbindin-D28K cells in the hamster SCN express light-induced Fos. Neuroreport 7:1224–1228.

Smale L, Boverhof J. 1999. The suprachiasmatic nucleus and intergeniculate leaflet of *Arvicanthis niloticus*, a diurnal murid rodent from East Africa. J Comp Neurol 403:190–208.

Smale L, Blanchard JH, Moore RY, Morin LP. 1991. Immunocytochemical characterization of the suprachiasmatic nucleus and the intergeniculate leaflet in the diurnal ground squirrel, *Spermophilus lateralis*. Brain Res 563:77–86.

Stellwagen D, Shatz CJ. 2002. An instructive role for retinal waves in the development of retinogeniculate connectivity. Neuron 33:357–367.

Stephan FK, Donaldson JA, Gellert J. 1982. Retinohypothalamic tract symmetry and phase shifts of circadian rhythms in rats and hamsters. Physiol Behav 29:1153–1159.

Turek FW, Losee-Olson S. 1986. A benzodiazepine used in the treatment of insomnia phase-shifts the mammalian circadian clock. Nature 321: 167–168.

Walker DL, Davis M. 1997. Double dissociation between the involvement of the bed nucleus of the stria terminalis and the central nucleus of the amygdala in startle increases produced by conditioned versus unconditioned fear. J Neurosci 17:9375–9383.

Wickland C, Turek FW. 1994. Lesions of the thalamic intergeniculate leaflet block activity-induced phase shifts in the circadian activity rhythm of the golden hamster. Brain Res 660:293–300.

Young MJ, Lund RD. 1997. The anatomical substrates subserving the pupillary light reflex in rats: origin of the consensual pupillary response. Neuroscience 62:481–486.

Youngstrom TG, Nunez AA. 1986. Comparative anatomy of the retinohypothalamic tract in photoperiodic and non-photoperiodic rodents. Brain Res Bull 17:485–492.

Zhang DX, Rusak B. 1989. Photic sensitivity of geniculate neurons that project to the suprachiasmatic nuclei or the contralateral geniculate. Brain Res 504:161–164.